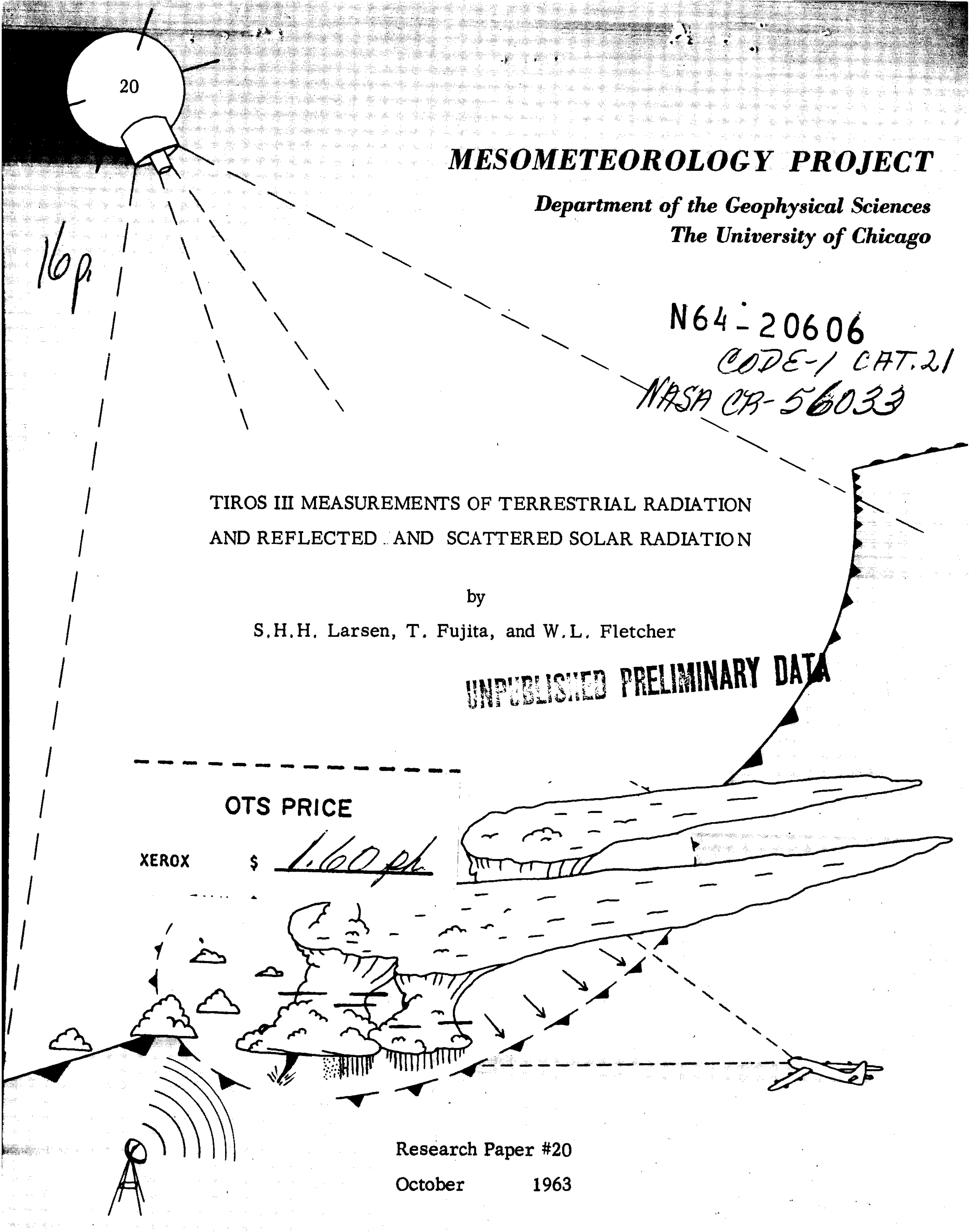

MESOMETEOROLOGY PROJECT

Department of the Geophysical Sciences
The University of Chicago

16p

N64-20606
CODE-1 CAT.21
NASA CR-56033

TIROS III MEASUREMENTS OF TERRESTRIAL RADIATION AND REFLECTED AND SCATTERED SOLAR RADIATION

by

S.H.H. Larsen, T. Fujita, and W.L. Fletcher

Research Paper #20
October 1963

MESOMETEOROLOGY PROJECT --------RESEARCH PAPERS

1. Report on the Chicago Tornado of March 4, 1961 - Rodger A. Brown and Tetsuya Fujita *

2. Index to the NSSP Surface Network - Tetsuya Fujita *

3. Outline of a Technique for Precise Rectification of Satellite Cloud Photographs - Tetsuya Fujita *

4. Horizontal Structure of Mountain Winds - Henry A. Brown *

5. An Investigation of Developmental Processes of the Wake Depression Through Excess Pressure Analysis of Nocturnal Showers - Joseph L. Goldman *

6. Precipitation in the 1960 Flagstaff Mesometeorological Network - Kenneth A. Styber *

7. On a Method of Single- and Dual-Image Photogrammetry of Panoramic Aerial Photographs - Tetsuya Fujita (To be published)

8. A Review of Researches on Analytical Mesometeorology - Tetsuya Fujita

9. Meteorological Interpretations of Convective Nephsystems Appearing in TIROS Cloud Photographs - Tetsuya Fujita, Toshimitsu Ushijima, William A. Hass, and George T. Dellert, Jr.

10. Study of the Development of Prefrontal Squall-Systems Using NSSP Network Data - Joseph L. Goldman

11. Analysis of Selected Aircraft Data from NSSP Operation, 1962 - Tetsuya Fujita

12. Study of a Long Condensation Trail Photographed by TIROS I - Toshimitsu Ushijima

13. A Technique for Precise Analysis of Satellite Data; Volume 1 - Photogrammetry - (Published as MSL Report No. 14) - Tetsuya Fujita

14. Investigation of a Summer Jet Stream Using TIROS and Aerological Data - Kozo Ninomiya

15. Outline of a Theory and Examples for Precise Analysis of Satellite Radiation Data - Tetsuya Fujita

* Out of Print

(Continued on back cover)

MESOMETEOROLOGY PROJECT

Department of the Geophysical Sciences

The University of Chicago

TIROS III MEASUREMENTS OF TERRESTRIAL RADIATION AND REFLECTED AND SCATTERED SOLAR RADIATION

by

S.H.H. Larsen*, T. Fujita, and W.L. Fletcher

RESEARCH PAPER #20

This research was supported by the National Aeronautic and Space Administration under grant NASA NsG 333, and partially by the Meteorological Satellite Laboratory, United States Weather Bureau, under grant Cwb WBG-6.

* On leave from Oslo University, Institute of Physics.

20606

ABSTRACT

A

The distribution of outgoing terrestrial radiation within the 8- to 12-micron band, over North Africa, is presented together with the pattern of reflected solar radiation. The analyses are based on data from analog traces of the five-channel medium resolution scanning radiometer on TIROS III. The data which have been used are obtained from measurements made under conditions favorable to the angular resolution of the radiometer, which changes as the satellite spins and progresses along its path; and a pattern of differential heating over the desert area was observed.

Calculations of the rate of reflectance over the Sahara desert have been made and the values obtained over the sand dunes, about 23 percent, appear to be realistic. These radiation data have also been used in a study of the anisotropic nature of scattered radiation; the results of this approach indicate the ability of the satellite to give valuable measurements in the study of scattering properties of the atmosphere.

AUTHOR

I. INTRODUCTION

The five-channel radiometers carried by the meteorological satellites (TIROS II, III, and IV) are scanning radiometers of medium resolution. Since the radiometer views the earth at different nadir angles, their resolution power varies as the satellite spins and progresses along its pass. In order to carry out research on physical interpretation of the radiation data obtained from the radiometer, it is necessary to determine the scanned areas where the resolution of the radiometer meets the standards required for our measurements.

In this paper, a satellite pass over Africa (R/O 101, 19 July 1961) has been selected for a detailed and careful analysis of the radiation data from Channels 2 and 3, which range from 8 to 12 microns and 0.25 to 6 microns respectively. On its pass, the satellite's radiometer scanned the Sahara desert, the semi-arid areas and the tropical wet areas near the equator, and the tropical wet and dry areas south of the equator at favorable nadir angles of view. The two synoptic patterns presented in Section II are derived from the satellite's radiation measurements over these regions, and they may give some information about the angular resolution of the radiometer; however, details in the structure of the synoptic pattern, which are significantly interpreted, are obtained by means of the precise rectification technique developed by Fujita (1963). The synoptic maps of terrestrial and reflected solar radiation show very clearly both a zone of intertropical convergence and a pattern of differential heating over the Sahara desert.

II. ANALYSIS OF TERRESTRIAL AND REFLECTED SOLAR RADIATION

The terrestrial upward radiation detected by the satellite's sensor is the energy filtered through the 8- to 12-micron Channel 2. Instrumental response may be converted into units of watts per square meter which expresses the filtered outgoing flux of isotropic radiation, and, if the value is denoted by $\overline{W}$, we may write

$$\overline{W} = \int_0^\infty W_\nu (T) \phi_\nu \, d\nu$$

where $\overline{W}$ is expressed as a filtered blackbody radiation. Tables from NASA (1962) are provided to convert the $\overline{W}$ into equivalent blackbody temperature; but, due to changes of the optical characteristics of the radiometer, correction has to be applied. The blackbody temperatures from Channel 2 measurements will approximate the surface or cloud top temperatures. Deviations appear for various reasons of which absorption within the spectral region of the channel may be the main one. A synoptic map of upward radiation as measured by the satellite on its pass over the north African continent on 19 July 1961 is shown in Fig. 1.

This analysis was actually used for the evaluation of limb darkening by Larsen, Fujita, and Fletcher (1963); however, it is shown here because some interesting features appeared due to the favorable resolution of the radiometer over these areas. On the map we find regions of extremely high values of outgoing radiation. They correspond to equivalent blackbody temperatures of about 38C to 40C, and coincide generally with those of the mountain areas in the Sahara. The temperatures measured over the sand dunes also show high values, but they usually range about five degrees lower. We see then, that an unexpected pattern of differential heating has been derived from satellite radiation measurements.

The upward reflected and scattered solar radiation is measured through Channel 3 (0. 25 to 6 microns), and the synoptic map shown in Fig. 2 is derived from such measurements. The scanned area is exactly the same as the previous one, and the values given in this case are also filtered flux values in watts per square meter. The mountain and the sand dune areas are indicated on the map where we find high values of reflected radiative energy over the sand dunes and lower over the mountains. This is a pattern different from that obtained by Channel 2 measurements of terrestrial heat radiation and a consequence of the difference in reflectivity within the wave lengths of Channel 3 spectral response.

These two maps shown in Figs. 1 and 2 give examples of the details one is able to detect if favorable conditions exist and a precise rectification technique is applied to the radiation data. In fact, to a certain extent we could map the sand dunes from Channel 3 measurements.

Farther south on the same maps, within the zone of intertropical convergence, we find very high values of reflected solar radiation and low values of terrestrial radiation. Within this area, showers and thunderstorms are reported; the spreading out of anvils from cumulonimbi into large areas of strato-formed cirrus probably accounts for the high values measured. A further examination using the topographic maps indicates that such large clouds with very great reflectivity do not exist over the region of high mountains.

III. REFLECTANCE

When the radiometer response is converted into flux values $\overline{W}$ where

$$\overline{W} = \int_0^\infty W_\nu(T)\,\phi_\nu\,d\nu,$$

an assumption about isotropic radiation can be made. However, the intensity of the radiation is implicit in a radiometer measurement, and in cases of isotropic radiation, the actual value would be $\overline{W}/\pi$; therefore, we may use the $\overline{W}$ values as a measure of the intensity of the radiation in the measured direction. If we now take the ratio between the reflected energy ($\overline{W}$) and the incoming solar radiation upon the horizontal surface, ($\overline{W}^* \cos\zeta_0$) both filtered flux values, this ratio ($\overline{W}/\overline{W}^* \cos\zeta_0$), where ζ_0 denotes the solar zenith angle, will be a measure of the reflectance reduced from one particular direction of observation by a satellite. The reflectance would be a characteristic of the reflecting surface itself. However, due to the influence of the atmosphere the measured $\overline{W}/\overline{W}^*\cos\zeta_0$ would depend on the direction of observation even though a perfectly diffuse reflector is considered. Dimensionally and numerically a measured value of $1/\pi \cdot \overline{W}/\overline{W}^{*}\cos\zeta_{o}$ would be a differential reflectance; and, when this is integrated over all directions, an apparent reflectance is obtained.

Calculations have been made and a synoptic map has been obtained from the values of $\overline{W}/\overline{W}^{*}\cos\zeta_{o} \cdot 100$. The values obtained over the sand dunes, 22 and 23 per cent, appear to be realistic values. The map is shown in Fig. 3.

In some cases the assumption of isotropic radiation may be a good approximation, but this is not always so. Several satellite measurements have been carefully selected in an attempt to learn if the satellite has the ability to indicate an anisotropy in the reflected and scattered radiation according to the laws governing molecular and non-molecular scattering of light. This attempt is described in the next section.

IV. OBSERVED ANISOTROPY OF REFLECTED AND SCATTERED RADIATION FROM CHANNEL 3 MEASUREMENTS

When incident solar radiation is reflected upward, this radiation is isotropic if the reflecting surface is a perfectly diffuse reflector. The earth's surface is not a perfectly diffuse reflector; furthermore the light scattered from the atmosphere also becomes part of the total energy measured by the radiometer. Channel 3 is a very broad channel (0. 25 to 6 microns), and both molecular and large particle scattering will contribute to the total amount of scattered and reflected light. In the case where the satellite scans clouds, the physical interpretation of the actual radiometer response represents a complex optical problem, and one would certainly not expect the upward radiation to be isotropic.

As a consequence of the TIROS satellite scan geometry, we are able to make two measurements (spanning a period of about ten minutes) of the upward radiation originating in a particular area. Usually such an area is viewed by the satellite at different zenith angles, but in order to keep constant some of the variable parameters which influence our measurements, we select scan spots where the satellite has the same zenith angle in its two different positions. Thus the path length for the upward radiation through the atmosphere will be the same; and, since the two measurements are taken within a time interval of a few minutes, the sun's zenith angle will be the same. By this selection, we are dealing with a pair of measurements where the back scattering angle (angle between the incident and outgoing beam) is different, but the other conditions remain the same. The geometry for such measurements, where the back scattering angle is the only parameter that varies, is shown in Fig. 4 .

On a base map, the positions of the scan spots fulfilling the condition of equal zenith angles were found on a line between 5S, 43E, and 14S, 30E. The area enclosing this line is scanned twice by the satellite: first by the initial scans and then by the complemental scans. The radiation data (from Channel 3) were analysed, and two separate synoptic maps of the reflected and scattered radiation were obtained from the same area. Along the line of equal zenith angles, the values of outgoing radiation were found from each of the two synoptic maps, and a cross section was constructed as shown in Fig. 5.

The scattering angles (or back scattering angles) were found by construction, using a method developed by Fujita, and the values are indicated on the cross section diagram and denoted by ψ_I' and ψ_C'. In these measurements, the plane of the satellite vertical and the scattered beam (TSC - SAT - TSP on Fig. 4) will not be in the local vertical sun plane through the scan spot. This will make an interpretation of the measurements more complex because the phenomenon is not axially symmetric due to the higher order of scattering. In our case we are not too far distant from the sun's vertical plane and some simple remarks will be made about these measurements.

As a consequence of the geometry of the space-oriented TIROS satellite, its scanning radiometer should never measure the forward scattering peak or the direct back scattering. Measurements made in the initial scans are, in this case, taken in a direction near the backward scattering point; and those from the complemental scan will be farther away from it ($\psi_I' < \psi_C'$).

From Dermendjian's work (1962) one would expect higher values from the initial scans, and the effect shown in the cross section is therefore encouraging, expecially if one looks at the western part of it. Probably there are no bright clouds over this part of the measured area, and a 17 percent increase in radiated energy is caused by the change in contributed scattered radiation.

In the eastern part of the scanned area, cumulus clouds appear; perhaps the main effect will be that the satellite first scans the sunlit part of the clouds. Then those parts of the clouds in the shadow are scanned. Nevertheless, such measurements over cloud covered areas would be more valuable if cloud pictures are taken at the same time. In our case no photographs were taken.

This approach may be valuable in that the results indicate the ability of satellite measurements to detect anisotropy in scattered radiation. However, additional information about the conditions in the scattering atmosphere are needed; and several similar cases should be studied before any general physical interpretation involving scattering processes is made on the basis of satellite measurements.

REFERENCES

Dermendjian, D., 1962: Scattering and polarization properties of polydispersed suspensions with partial absorption. The Rand Corporation, Santa Monica, California.

Fujita, T., 1963: Outline of a theory and examples for precise analysis of satellite radiation data. Mesometeorology Research Paper No. 15, University of Chicago.

Larsen, S.H.H., T. Fujita, W.L. Fletcher, 1963: Evaluation of limb darkening. Mesometeorology Research Paper No. 18, University of Chicago.

NASA, 1962: TIROS III radiation data user's manual. Goddard Space Flight Center, Greenbelt, Maryland.

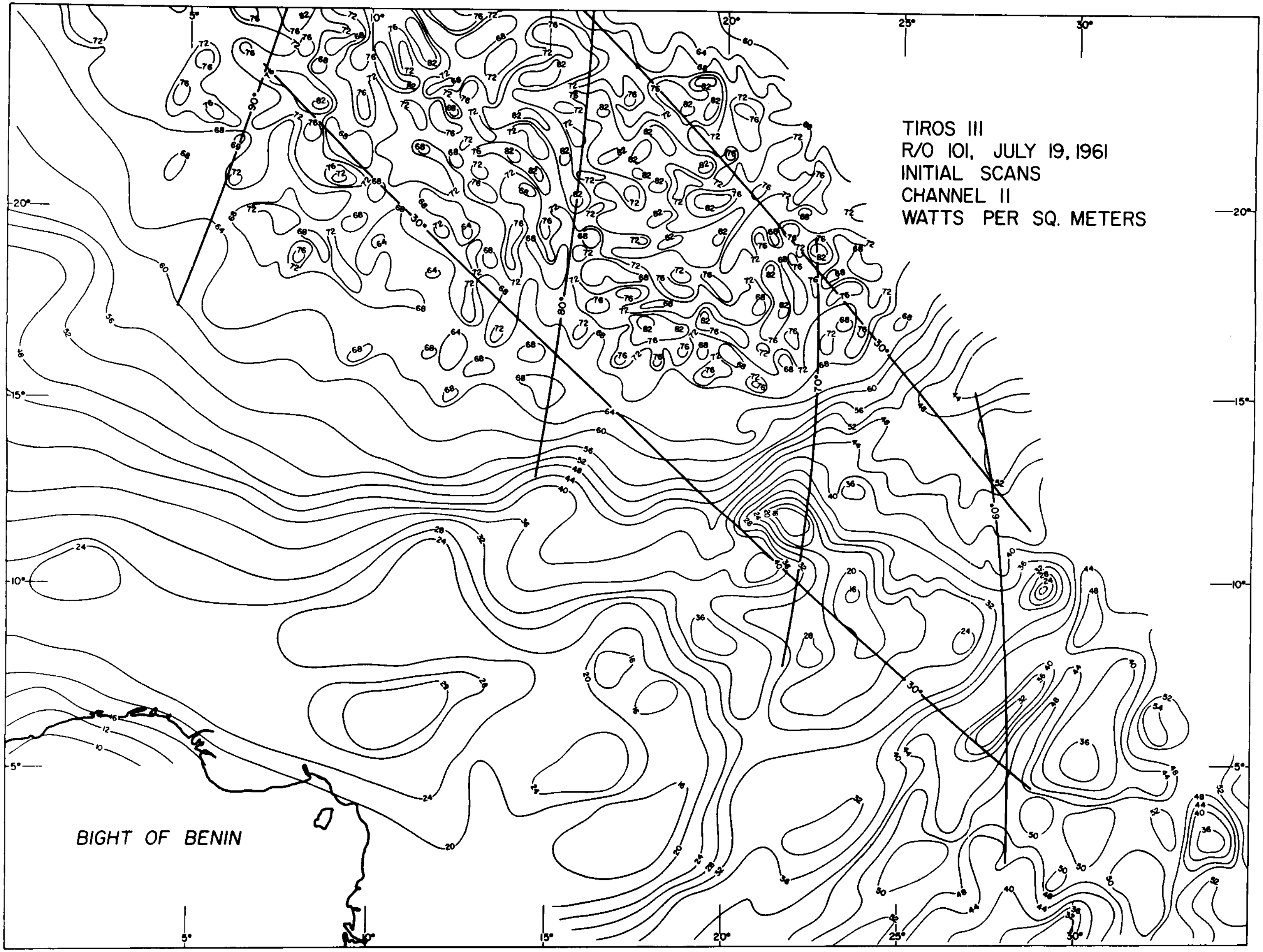

Fig. 1. Distribution of outgoing terrestrial radiation measured between 1012 and 1022 GCT, 19 July 1961. The chart may be considered synoptic. The heavy curves over the scanned area denote the zenith angles of the initial scans (30) and those of the complemental ones (60 to 90).

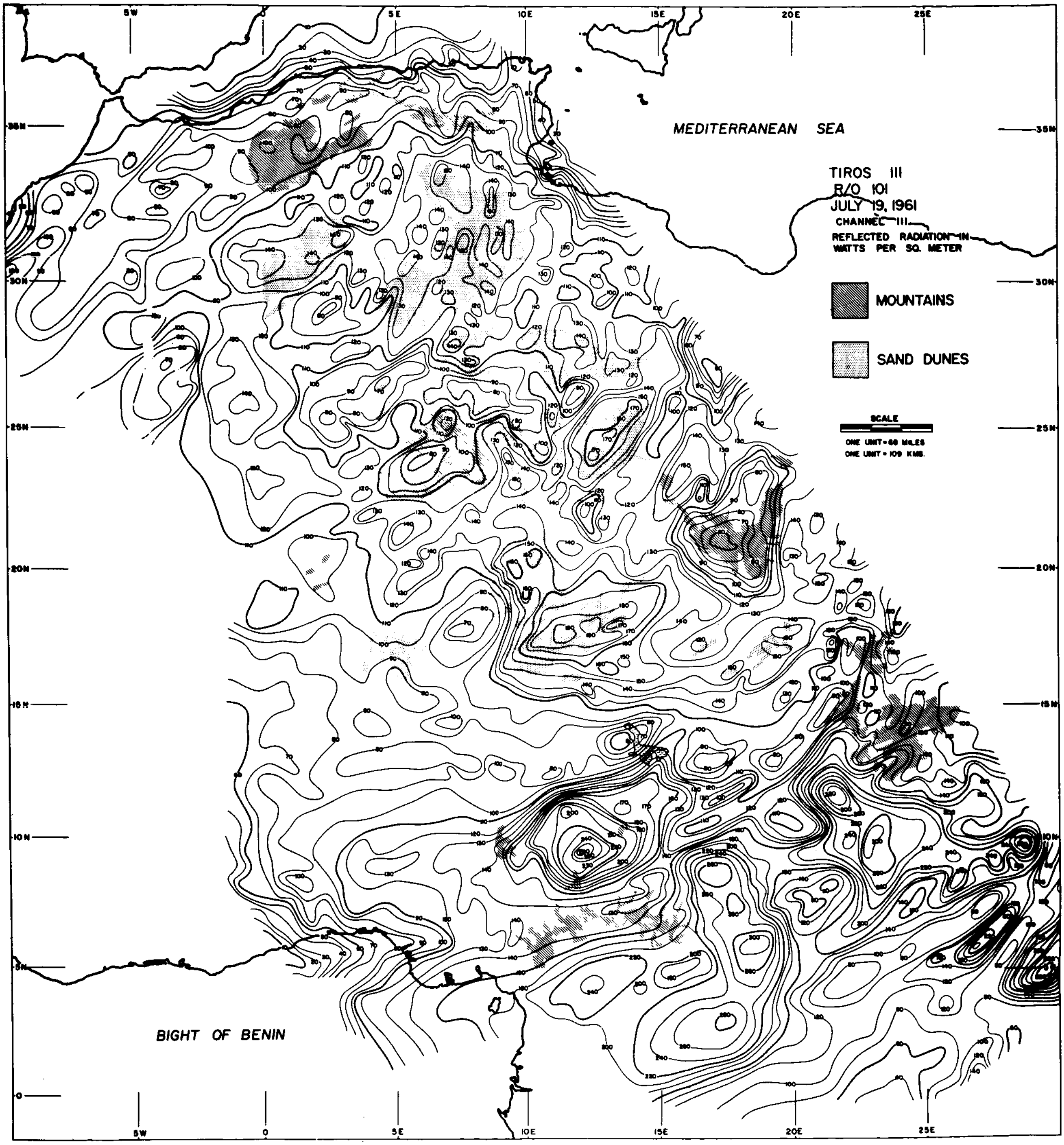

Fig. 2. Synoptic map of reflected and scattered solar radiation based on satellite measurements in the 0.25 to 6 micron region. Very high values are observed from clouds within the zone of intertropical convergence.

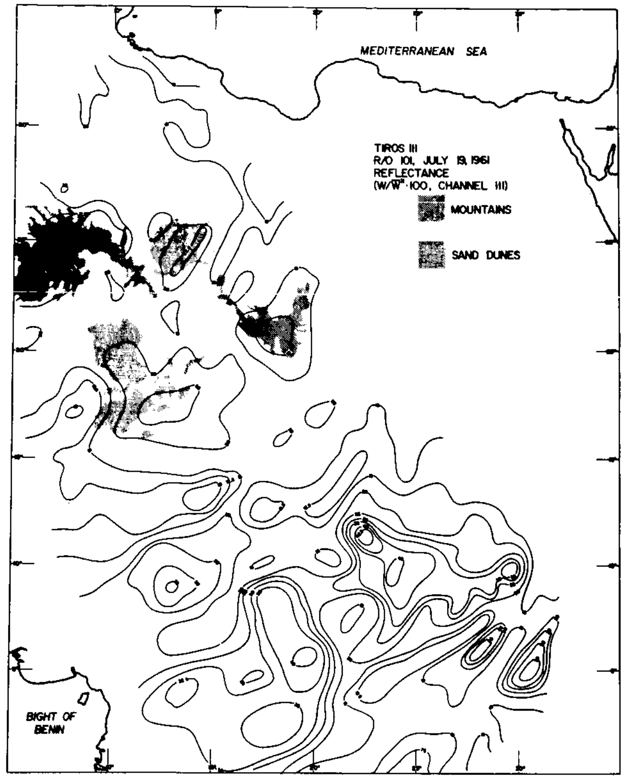

Fig. 3. Synoptic map of reflectance expressed as percent reflected radiative energy.

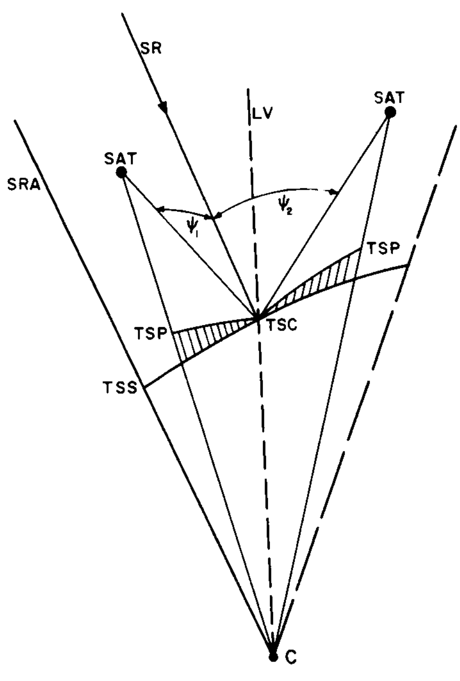

Fig. 4. The geometry in situations where scattered radiation, originating within the same area, reaches the satellite in its two positions at the same zenith angles as the scattering angles are different. Notation; TSS: Terrestrial Sub Solar point. SR: Sun Ray. TSC: Terrestrial Scan Spot. SAT: Satellite.

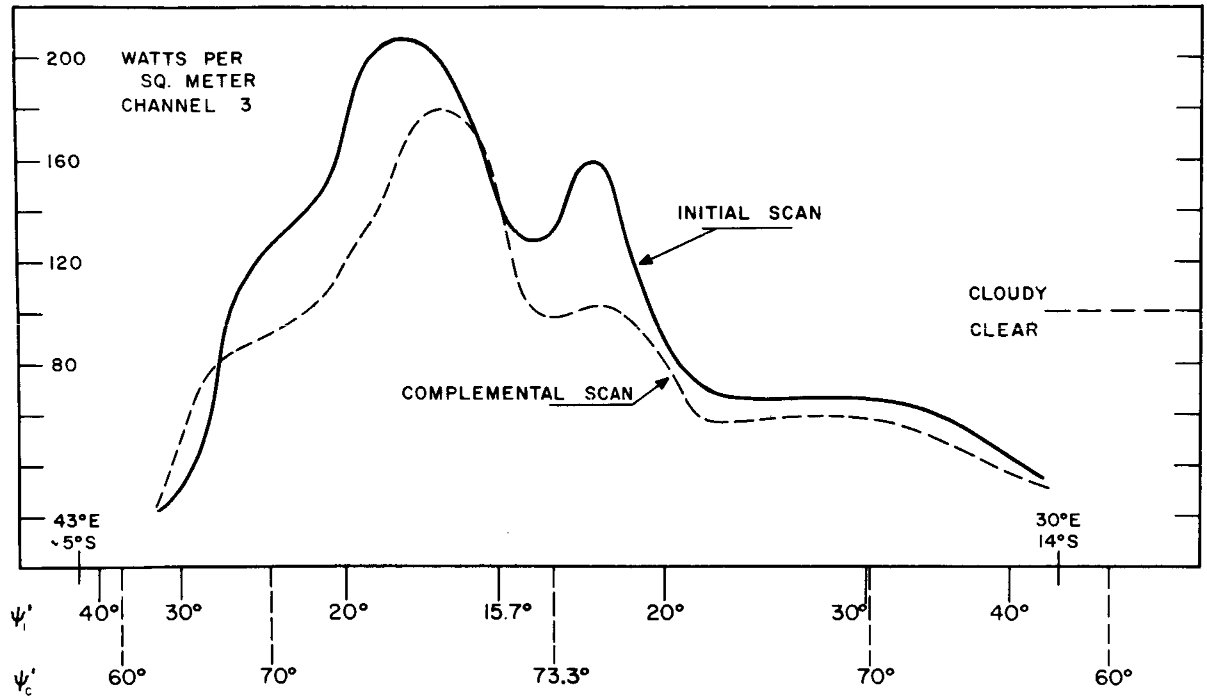

Fig. 5. Observed change in amount of outgoing scattered radiation. The IS-curve represents values of radiation scattered at small back-scattering angles, ψ_I' : and the CS-curve represents values of radiation scattered at large back-scattering angles, ψ_C' .

MESOMETEOROLOGY PROJECT -------- RESEARCH PAPERS

(Continued from front cover)

16. Preliminary Result of Analysis of the Cumulonimbus Cloud of April 21, 1961 - Tetsuya Fujita and James Arnold

17. A Technique for Precise Analysis of Satellite Photographs - Tetsuya Fujita

18. Evaluation of Limb Darkening From TIROS III Radiation Data - S. H. H. Larsen, Tetsuya Fujita, and W. L. Fletcher

19. Synoptic Interpretation of TIROS III Measurements of Infrared Radiation - Finn Pedersen and Tetsuya Fujita